PHYSICAL REVIEW B **104**, 155148 (2021)

$5f$-electron magnetism in single crystal UN probed by ^{14}N NMR

V. V. Ogloblichev,[1,*] S. V. Verkhovskii,[1] A. V. Mirmelstein,[2] Y. V. Piskunov,[1] A. Y. Germov,[1]
A. M. Potapov,[3] A. F. Gubkin,[1,4] and A. V. Andreev[5]
[1]*M. N. Mikheev Institute of Metal Physics of Ural Branch of Russian Academy of Sciences, Yekaterinburg 620108, Russia*
[2]*FSUE "RFNC-VNIITF named after Academician E. I. Zababachin," Snezhinsk 456770, Chelyabinsk region, Russia*
[3]*Institute of High-Temperature Electrochemistry of Ural Branch of Russian Academy of Sciences, Yekaterinburg 620990, Russia*
[4]*Institute of Natural Sciences and Mathematics, Ural Federal University, Yekaterinburg 620002, Russia*
[5]*FZU Institute of Physics, Czech Academy of Sciences, Prague 18221, Czech Republic*

(Received 12 December 2020; revised 11 August 2021; accepted 30 September 2021; published 27 October 2021)

Spin susceptibility and low-frequency dynamics of uranium $5f$ electrons have been investigated by nuclear magnetic resonance (NMR) on the ^{14}N nuclei in paramagnetic and magnetically ordered phases for single crystalline and polycrystalline samples of uranium mononitride (UN). NMR spectra, shifts of the ^{14}N NMR lines, and the spin-lattice relaxation times T_1 have been obtained in the temperature range $T = 10$–$760\,$K in magnetic field $B = 92.8\,$kOe. It is shown that in the UN paramagnetic phase, temperature dependence of the ^{14}N NMR line shift is proportional to the spin susceptibility of the uranium $5f$ electrons. Joint analysis of NMR and magnetic susceptibility data allows us to determine temperature dependence of spin fluctuation energy $\Gamma_{\mathrm{nmr}}(T)$ of the uranium $5f$ electrons and to demonstrate that its temperature variation is close to $\Gamma(T) \propto T^{0.5}$ dependence which is characteristic of the concentrated Kondo systems above the coherent state formation temperature. In the magnetically ordered UN phase the ^{14}N NMR spectra consist of several lines that can be explained in terms of the model of type *I* antiferromagnetic order corresponding to $1k$ structure in the presence of magnetic domains.

DOI: 10.1103/PhysRevB.104.155148

I. INTRODUCTION

Uranium mononitride (UN) is a representative of the actinide compounds with metallic conductivity where the $5f$ electrons demonstrate the peculiarities of both local and band magnetism [1–6]. For more than half a century the fundamental problem of such dual behavior of the $5f$ electrons in this prospective material remains in the center of experimental and theoretical investigations.

In the UN face-centered cubic lattice of NaCl-type ($Fm3m$ space group) the uranium interatomic distance $d_{\mathrm{U-U}} = 3.45\,$Å [4] is close to but less than the Hill criterion value $d_{\mathrm{Hill}} = 3.5\,$Å [7]. Thus this compound should be considered as a system of itinerant $5f$ electrons. The results of angle-resolved photoemission spectroscopy (ARPES) [8] experiments in magnetically ordered phase under pressure [9], and recent local density approximation plus dynamical mean field theory (LDA+DMFT) calculations of the UN electron structure for the paramagnetic phase [10,11] lead to the same conclusion. At the same time, the authors of [10] describe UN as "a strongly correlated bad metal" having in mind the dominant contribution of electron-electron scattering to the temperature dependence of electrical resistivity, which is usually observed in the temperature range of the incoherent regime of electron fluctuations in the concentrated Kondo systems [12]. In the paramagnetic phase the UN magnetic susceptibility follows the Curie-Weiss dependence with negative paramagnetic Curie temperature and effective moment $\mu_{\mathrm{eff}} = 2.3$–$2.7\,\mu_{\mathrm{B}}$ [1,13,14]. Traditionally, this is considered as evidence for local magnetism in uranium mononitride. Below 53 K in UN a commensurate antiferromagnetic (AF) structure [type $1k$; $\mathbf{k}_{\mathrm{AF}} = (0\,0\,1)$] with an anomalously small value of the sublattice magnetic moment $\mu_{\mathrm{ord}} = 0.75\mu_{\mathrm{B}}$ [15] is formed. Explanation of such a big difference between μ_{ord} and μ_{eff} as a result of the crystal field effect [16] is not confirmed by the inelastic neutron scattering experiments [17], according to which no signs of transverse magnetic excitations are found in UN up to frequencies of 10 THz. Moreover, above 30 K a rapid increase in the intensity of quasielastic scattering near the structural Bragg peaks is observed. Most probably, the origin of this feature is connected with coupled charge and magnetic fluctuations of the uranium ions.

The effectiveness of $^{14(15)}$N NMR as a tool for investigation of the UN magnetic properties has been long known due to the innovative research [18,19] performed in Argonne National Laboratory in the 1970s. The results of our brief NMR investigation are published in Ref. [20], where the dynamic behavior of the uranium $5f$-electron magnetic moment in the paramagnetic phase of the polycrystalline UN sample is studied by measuring nuclear spin-lattice relaxation rate T_1^{-1} of the ^{14}N nuclei in the temperature range $1.5T_{\mathrm{N}} < T < 7T_{\mathrm{N}}$. It is shown that spin fluctuation energy $\Gamma_{\mathrm{nmr}}(T)$ of the $5f$ electrons increases gradually with increasing temperature following the dependence close to $\Gamma(T) \propto T^{0.5}$ observed in concentrated

---

[*] Present address: M. N. Mikheev Institute of Metal Physics of Ural Branch of Russian Academy of Sciences (IMP UB RAS), Kovalevskaya Strasse 18, 620108 Yekaterinburg, Russia; ogloblichev@imp.uran.ru

Kondo systems above the coherent state formation temperature [12,21].

This work presents the measurement results of magnetic susceptibility, the ^{14}N NMR line shift, and spin-lattice relaxation time of the ^{14}N nuclei in paramagnetic and AF phases of the UN single crystal within the temperature range $10 < T < 380$ K. Additionally, the detailed NMR data for temperatures up to 760 K are presented in order to identify the uranium charge and spin states in UN at the temperatures of its possible practical application as an advanced fuel for nuclear power engineering. These data are obtained using the same polycrystalline UN sample as in Ref. [20].

II. SAMPLES AND EXPERIMENTAL DETAILS

The UN single crystal, 54 mg in mass, belongs to a single crystal series characterized and studied in Refs. [5,22,23]. The polycrystalline UN sample has the form of a cylinder, 5 mm in diameter, 6 mm in height, and 1.8 g in mass.

The ^{14}N NMR experiments were performed using the homebuilt pulse NMR spectrometer in the external magnetic field $B = 92.8\,\text{kOe}$ within the temperature ranges from 10 to 380 K and from 60 to 760 K for the single crystal and polycrystalline sample, respectively.

The single crystal was packed in a plastic container and installed in the correct orientation for measurement inside the rf coil (solenoid with a diameter of 4 mm) of the low-temperature NMR sensor. The cylindrical polycrystalline sample was placed into the quartz vessel and packed firmly with quartz sand. The quartz vessel was placed inside the radio-frequency coil (solenoid with a diameter of 7 mm) of the high-temperature homebuilt NMR sensor. The low-temperature and high-temperature sensors with samples were placed inside a CF1200 cryostat (Oxford Instruments, UK) with constant cooling gas flow (N_2 or He for temperatures $T < 80$ K). In all the experiments the sample temperature ($\Delta T/T \leqslant 0.05$) was measured and stabilized by an ITC5 temperature controller (Oxford Instruments, UK), equipped with thermocouples (Cu-Au:Fe07) or chromel/alumel placed close to the sample in the resonance probe.

The NMR ^{14}N spectra were obtained using standard spin-echo procedure p–t_{del}–p–t_{del}–*echo*. The duration of the first pulse was $p = 2.6\,\mu\text{s}$ and the power of the rf amplifier was 400 W. The ^{14}N NMR spectra are the Fourier transforms of the measured *echo* signal. While recording spectra with width exceeding the frequency band excited by the rf pulse, the summation procedure was applied to the array of signals accumulated within the required frequency range with a step of $\Delta\nu = 60\,\text{kHz}$. The delay between pulses t_{del} was 250 μs. Shifts of the NMR lines $K = (\nu\text{–}\nu_0)/\nu_0$ were detected with reference to Larmor frequency $\nu_0 = 28.542$ MHz of the ^{14}N nuclei in an ammonia solution at room temperature.

Spin-lattice relaxation time T_1 was measured by the inversion-recovery method of nuclear magnetization using the pulse sequence $2p$–t_{inv}–p–t_{del}–p–t_{del}–*echo* at constant delay $t_{\text{del}} = 200\,\mu\text{s}$ in the interval $t_{\text{inv}} = (0.01\text{–}10)T_1$. Above 400 K the T_1^{-1} measurements were carried out using the pulse sequence p–t_{del}–p–t_{del}–*echo* with fixed t_{del} and variable repetition time of the pulse sequence $t = t_{\text{inv}} = 0.01\text{–}2$ s. Spin-lattice relaxation times were well described by the exponential dependence $[M_0 - M(t_{\text{inv}})] \propto \exp(-t_{\text{inv}}T_1^{-1})$, where M_0 is the equilibrium nuclear magnetization of spin system $t_{\text{inv}} \geqslant 5T_1$, and $M(t_{\text{inv}})$ is the nuclear magnetization at time t. The examples of $M(t_{\text{inv}})$ fitting to data for monocrystalline and polycrystalline samples at different temperatures are shown in the inset of Fig. 6(a).

Magnetic susceptibility χ is measured on the UN single crystal using a MPMS-XL-5 SQUID magnetometer (Quantum Design, USA) in magnetic field $B = 30\,\text{kOe}$ within the temperature range $2 \leqslant T < 320$ K. Magnetic susceptibility of the polycrystalline sample is measured using the same equipment and presented in Ref. [20].

III. RESULTS AND DISCUSSION

A. ^{14}N NMR line shift and magnetic susceptibility

Figure 1 shows evolution of the ^{14}N NMR spectra as a function of temperature in the paramagnetic phase for the single crystalline and polycrystalline UN samples. The ^{14}N nucleus has an integer spin $I = 1$, gyromagnetic ratio $\gamma_n = \gamma/2\pi = 0.3075\,\text{MHz/kOe}$, and nuclear quadrupole moment $Q = 20.44$ mb [24]. Therefore, in general both nuclear Zeeman transitions $m_I = +1 \leftrightarrow 0$ and $m_I = 0 \leftrightarrow -1$ are split due to the quadrupole interaction eQ between the ^{14}N nucleus and electric field gradient eV_{zz} (EFG), produced in the nucleus location by its charge neighbor [25,26]. As soon as UN has a cubic structure, splitting of the ^{14}N NMR spectrum line into two components does not occur [24–26]. The NMR spectrum for the UN single crystal is a narrow single line with a full width at half maximum of $\Delta\nu \approx 14\,\text{kHz}$ for external magnetic field $\mathbf{B} \parallel [001]$ and $\Delta\nu \approx 5\,\text{kHz}$ for $\mathbf{B} \parallel [111]$ (Fig. 1). This difference can be caused by slight imperfection of the single crystal which results in the appearance of the quadrupole interaction between the ^{14}N nuclei and EFG [27]. Besides, different linewidths of the NMR lines may be connected with distribution of the dipole fields produced by the U ions at nitrogen positions. However, these fields are zero in the paramagnetic state of a cubic crystal lattice.

In fact, the ^{14}N NMR lines of the UN single crystal are extremely narrow and we can conclude that distortions of cubic symmetry of the charge neighborhood of nitrogen atoms are insignificant.

Therefore, in the paramagnetic region of the UN single crystal all the nitrogen sites are magnetically equivalent and the charge distribution on neighboring sites has a cubic symmetry. The ^{14}N NMR line broadening is much more pronounced in the polycrystalline sample [Fig. 1(c)] due to the random orientations of the crystallites in the powder [20].

Figure 2 shows temperature dependencies of the ^{14}N NMR line shift $K = (\nu\text{–}\nu_0)/\nu_0$ in the paramagnetic phase. Resonance frequency ν is determined by the position of the NMR line peak in a single crystal and by the center of gravity in the polycrystalline UN sample [20]. Very narrow lines observed in the single crystal lead to the error $\Delta K/K \leqslant 3 \times 10^{-3}$, which becomes comparable with the accuracy of magnetic susceptibility χ data (Fig. 3). The behavior of shift $K(T)$ is satisfactorily described by the Curie-Weiss dependence $K(T) = K_0 + C/(T\text{–}\theta_{\text{nmr}})$. Above 80 K the fitting parameters are $K_0 = 0.02(4)\%$ and $\theta_{\text{nmr}} = \text{–}210(20)$ K.

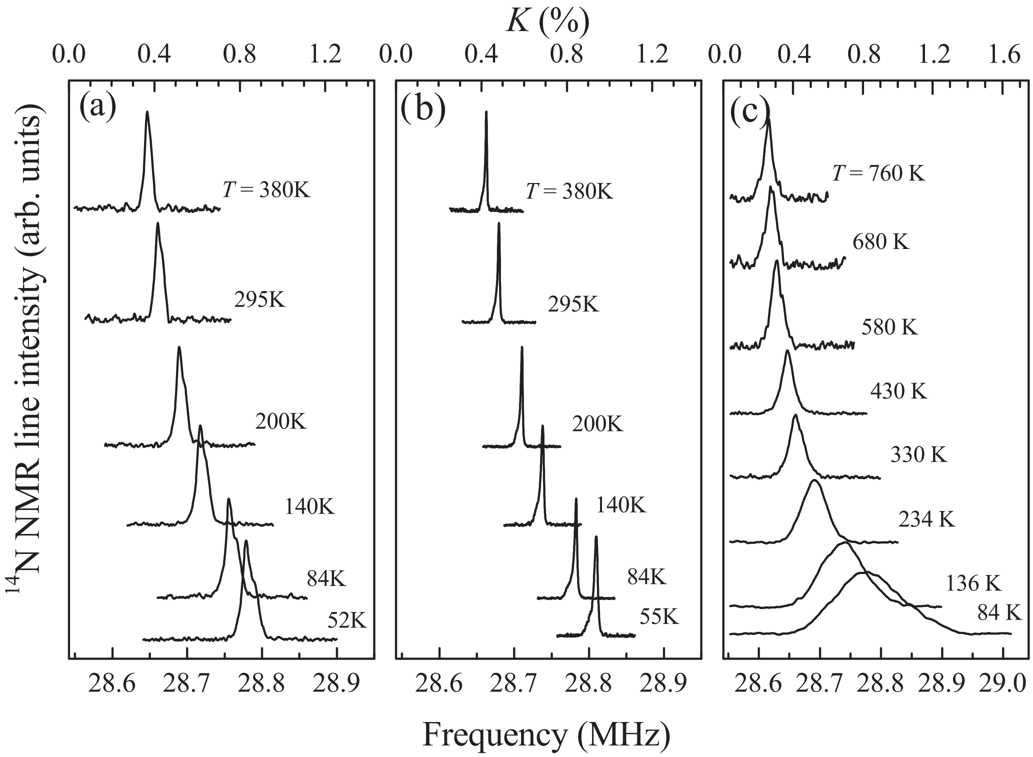

FIG. 1. The ^{14}N NMR spectra in the paramagnetic phase of UN in magnetic field $B = 92.8\,\mathrm{kOe}$ measured for (a) single crystal in magnetic field $\mathbf{B} \parallel [001]$, (b) single crystal in magnetic field $\mathbf{B} \parallel [111]$, and (c) polycrystalline sample. The reference point $K = 0$ for NMR line shift corresponds to the frequency $\nu_0 = 28.542\,\mathrm{MHz}$.

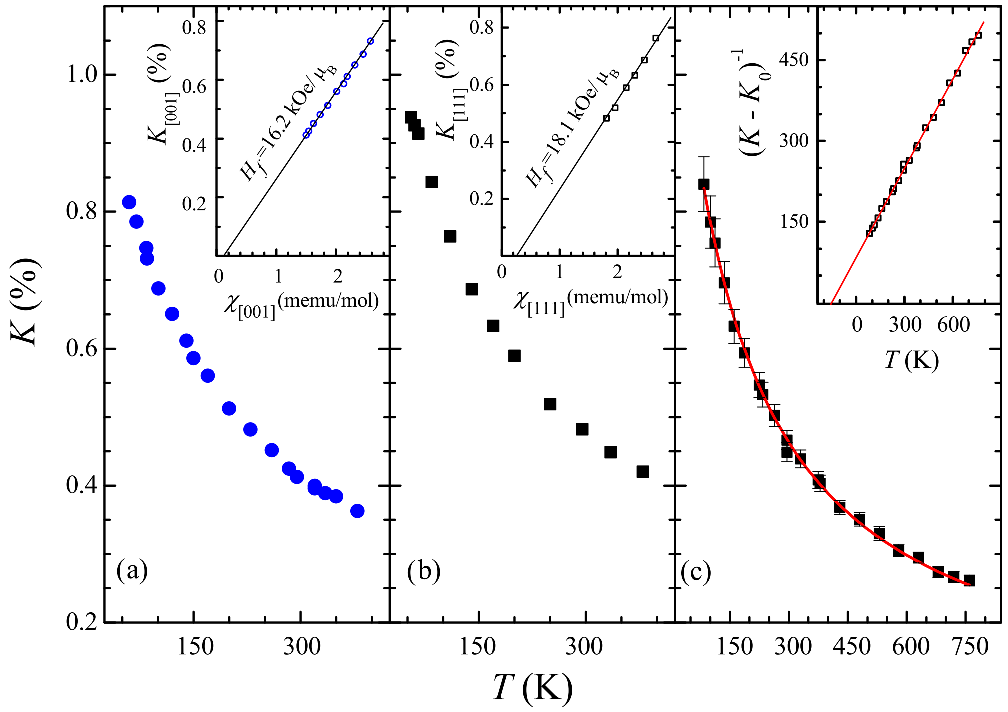

FIG. 2. Temperature dependence of the ^{14}N NMR line shift K in the UN paramagnetic phase measured for (a) single crystal in magnetic field $\mathbf{B} \parallel [001]$, (b) single crystal in magnetic field $\mathbf{B} \parallel [111]$, and (c) polycrystalline sample. Insets in the panels (a), (b) show the parametric K vs χ dependence (open signs) and the fit of a straight line to experimental data. The inset in panel (c) shows the inverse shift $(K - K_0)^{-1}$ as a function of temperature (open signs). Solid lines represent fit of the experimental data by the Curie-Weiss dependence.

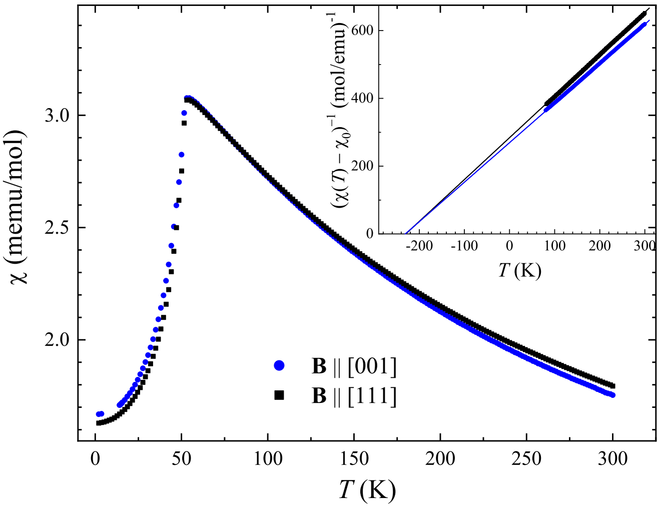

FIG. 3. Magnetic susceptibility χ vs temperature T for the UN single crystal measured in magnetic field $B = 30\,\mathrm{kOe}$ for $\mathbf{B} \parallel [001]$ (circles) and $\mathbf{B} \parallel [111]$ (squares). The inset shows T dependence of the inverse magnetic susceptibility $[\chi(T) - \chi_0]^{-1}$. Solid lines correspond to the fit of a straight line to experimental data above 80 K.

For the polycrystalline UN sample the temperature interval of $K(T)$ measurements is extended up to 760 K [Fig. 2(c)]. As seen, T dependence of $K(T)$ also follows the Curie-Weiss law with $\theta_{\mathrm{nmr}} = -155(10)\,\mathrm{K}$. This value coincides with the paramagnetic Curie temperature θ derived previously from the magnetic susceptibility measurements for this sample [20]. The temperature-independent contribution to the shift $K_0 = 0.06(4)\%$ is close to the values of the Knight shift for the nitrogen nuclei in nonmagnetic metallic thorium mononitride $K(\mathrm{Th}\,^{14}\mathrm{N}) = 0.107(30)\%$ [28] and $K(\mathrm{Th}\,^{15}\mathrm{N}) = 0.088(6)\%$ [29].

Figure 3 shows the temperature dependence of magnetic susceptibility χ measured in external magnetic field $B = 30\,\mathrm{kOe}$ using the same UN single crystal as for the NMR experiments. For these measurements a magnetic field is applied along two crystallographic directions of the UN single crystal, namely, $\mathbf{B} \parallel [111]$ and $\mathbf{B} \parallel [001]$. Maximum values of $\chi_{[111]}(T)$ and $\chi_{[001]}(T)$ are found at $T_{\mathrm{N}} = 51(1)\,\mathrm{K}$, indicating transition to the AF phase. Above 80 K the $\chi(T)$ behavior is satisfactorily described by the Curie-Weiss law, $\chi(T) = \chi_0 + C/(T - \theta)$, with Curie constant $C = 0.90(2)\,\mathrm{emu\,K/mole}$ and paramagnetic Curie temperature $\theta = -230(20)\,\mathrm{K}$. The corresponding effective magnetic moment calculated as $\mu_{\mathrm{eff}} = [C3k_{\mathrm{B}}/\mu_{\mathrm{B}}^2 N_{\mathrm{A}}]^{1/2} = 2.7\,\mu_{\mathrm{B}}$ is by one-third less than $\mu_{\mathrm{eff}} \approx 3.6\,\mu_{\mathrm{B}}$ for U^{4+} ($5f^2$, $J = 4$, $g_J = 0.8$) and U^{3+} ($5f^3$, $J = 9/2$, $g_J = 8/11$) configurations. The temperature-independent contribution $\chi_{0,[111]} = 2.6(1) \times 10^{-4}$ emu/mole exceeds the value of $\chi_{0,[001]} = 1.5(1) \times 10^{-4}$ emu/mole by a factor of $\sim$1.5. The origin of such an unusual χ_0 anisotropy can be understood while measuring $\chi(T)$ up to higher temperatures [13,14]. It should be noted that the single crystalline values of μ_{eff} and $|\theta|$ derived from our measurements are close to the corresponding values of $\mu_{\mathrm{eff}} \approx 2.6\,\mu_{\mathrm{B}}$ and $|\theta| > 200\,\mathrm{K}$ obtained for the nominally stoichiometric UN [1,13,14,30]. Meanwhile, lower values of $\mu_{\mathrm{eff}} \approx 2.4\,\mu_{\mathrm{B}}$ and $|\theta| \approx 160\,\mathrm{K}$ and bigger $\chi_0 = 3.5(1) \times 10^{-4}$ emu/mole for the polycrystalline UN sample can be caused by the presence of a small amount of molybdenum and carbon $m_{\mathrm{C}}/m_{\mathrm{U}} < 5 \times 10^{-4}$ [20,31]. These impurities acting as substitutional defects may promote delocalization of the uranium f electrons. As for the difference between the experimental $\sim$2.7 μ_{B} and expected $\sim$3.6 μ_{B} values of μ_{eff}, various explanations have been previously suggested. Lemmer and Lowther describe reduction of the localized U moment in terms of the crystalline electric field effects [32]. However, as mentioned above, inelastic neutron scattering experiments [17] revealed no signs of the transverse magnetic (crystalline electric field or magnonlike) excitations in UN up to 40 THz of frequencies at $T < 300$ K. Alternatively, Lukoyanov and Anisimov consider UN as an itinerant f-electron system and explain the experimental value of μ_{eff} as a result of mixing $j = 5/2$ and $j = 7/2$ configurations [11]. Following Hasegawa and Moriya [33], Fujimori *et al.* [8] directly relate the Curie-Weiss behavior above T_{N} in UN with the itinerant nature of the U $5f$ electrons.

The $^{14}\mathrm{N}$ NMR line shift in UN is governed by the hyperfine interactions of nuclear spin I with the electronic environment. Fermi contact interaction with the conduction band electrons $\gamma_n \hbar A \mathbf{I}\mathbf{S}^c$ is responsible for the temperature-independent contribution K_0. The effect of the uniform spin polarization of the conduction band electrons through the indirect electron-nuclear interactions with more localized f-electron spins is taken into consideration in the form of additive contribution $K_f(T)$ to the total shift [34,35]:

$$K(T) = K_0 + K_f(T) = K_0 + H_f \chi_f(T)/\mu_{\mathrm{B}} N_{\mathrm{A}}, \qquad (1)$$

where constant H_f has physical meaning of the effective hyperfine field, induced on nitrogen nuclei by the $5f$-shell electrons of the neighbor uranium ions, N_{A} is the Avogadro number, and $\chi_f(T)$ is the mole spin susceptibility of the uranium $5f$ electrons.

Thus, within the temperature range of the UN paramagnetic phase, proportionality $K(T) \propto \chi_f(T)$ can be expected. Actually, the parametric dependence $K(T)$ vs $\chi(T)$ above T_{N} confirms the applicability of relation (1) to describe the local moment magnetism of the $5f$ electrons in UN [Figs. 2(a) and 2(b)]. In the paramagnetic range the dependencies $K(\chi)$ are satisfactorily described by linear dependence with constants $H_{f,[001]} = 16.2(8)\,\mathrm{kOe}/\mu_{\mathrm{B}}$ and $H_{f,[111]} = 18.1(8)\,\mathrm{kOe}/\mu_{\mathrm{B}}$. Therefore, we determined that the main contribution to the nitrogen NMR line shift and total magnetic susceptibility in the UN paramagnetic phase is connected with local moment magnetism of the $5f$ electrons of uranium.

B. Magnetically ordered phase

Below $T_{\mathrm{N}} = 51\,\mathrm{K}$ the $^{14}\mathrm{N}$ NMR spectra become more complicated. Figures 4(a) and 5(a) show the $^{14}\mathrm{N}$ NMR spectra of UN obtained for two directions of magnetic field. The spectrum consists of three well-resolved lines, 1, 2, 3, at $\mathbf{B} \parallel [001]$, whereas at $\mathbf{B} \parallel [111]$ the spectrum is split into two lines, 4 and 5. In magnetically ordered phase, the $^{14}\mathrm{N}$ NMR spectrum shape is determined by the distribution over the crystal of the projection $\mathbf{h}_{\mathrm{loc}}(\mathbf{R})$ onto the direction of the external magnetic field $\boldsymbol{H}$, where $\mathbf{h}_{\mathrm{loc}}(\mathbf{R}) = \Sigma_i \mathbf{h}_{\mathrm{loc}}(\mathbf{r}_i)$ is the vector sum of local magnetic fields $\mathbf{h}_{\mathrm{loc}}(\mathbf{r}_i)$ created by magnetic moments of the

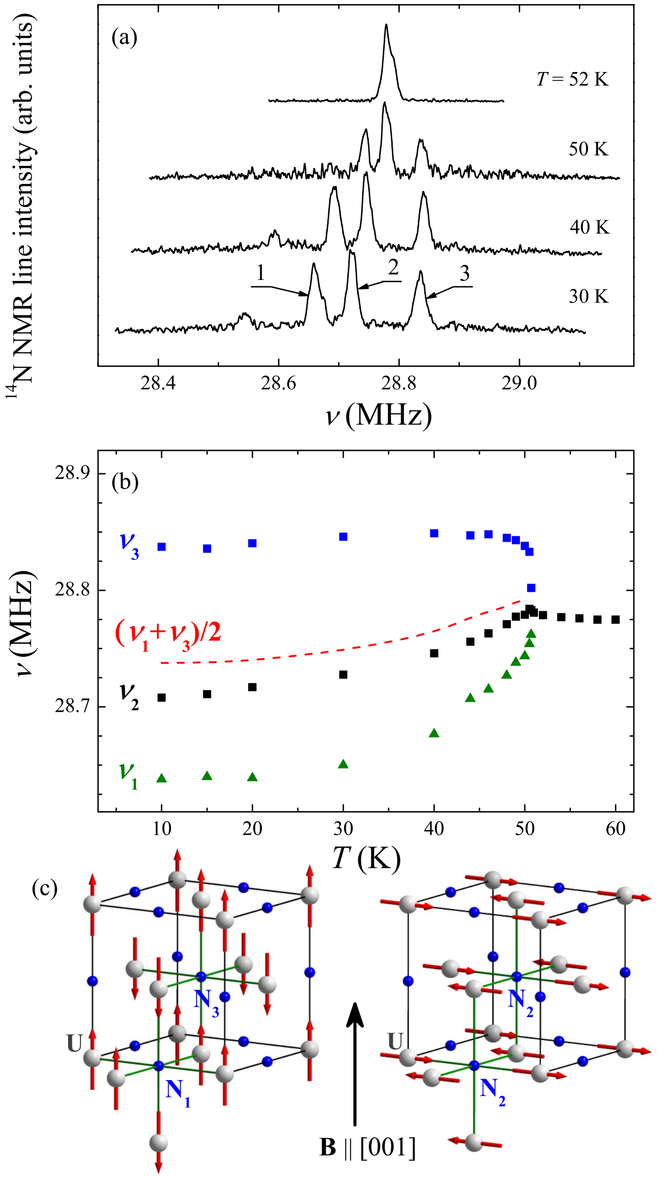

FIG. 4. (a) The ^{14}N NMR spectra for the UN single crystal in magnetic field **B** ∥ [001] below T_N. (b) Frequencies ν_i $(i = 1, 2, 3)$ of the NMR lines as a function of temperature. (c) Schematic view of magnetically nonequivalent nitrogen positions at magnetic field **B** ∥ [001] in the 1*k* type of the UN AF structure.

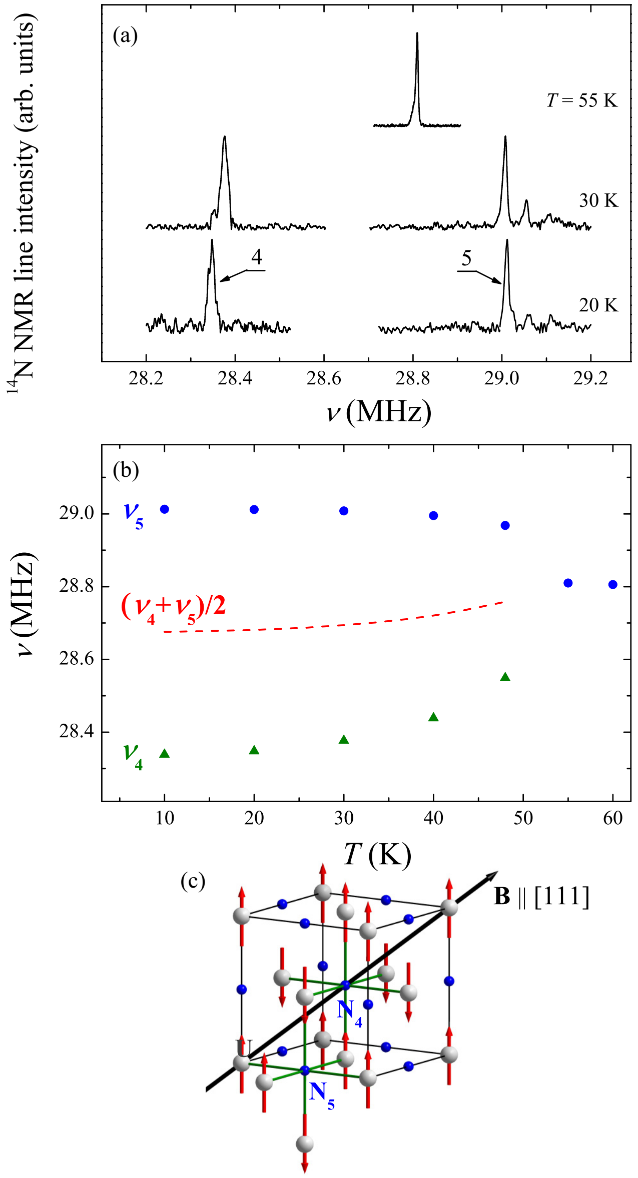

FIG. 5. (a) The ^{14}N NMR spectra for the UN single crystal in magnetic field **B** ∥ [111] below T_N. (b) Frequencies ν_i $(i = 4, 5)$ of the NMR lines as a function of temperature. (c) Schematic view of magnetically nonequivalent nitrogen positions at magnetic field **B** ∥ [111] in the 1*k* type of the UN AF structure.

uranium ions with radius vectors $\mathbf{r}_i$ at nitrogen positions **R**. In a simple case the local field on the nucleus of the nonmagnetic nitrogen ion is determined both by the dipole field $\mathbf{H}_{\text{dip}}$ produced by magnetic moments of the uranium ions and by the hyperfine field $\mathbf{H}_{\text{hf}}$ connected with transfer of spin polarization from the nearest magnetic neighbors:

$$\mathbf{H}_{\text{loc}} = \mathbf{H}_{\text{dip}} + \mathbf{H}_{\text{hf}} = \sum_i (\mathbf{h}_{\text{dip},i} + \mathbf{h}_{\text{hf},i}). \qquad (2)$$

Here $\mathbf{h}_{\text{dip},i}$ and $\mathbf{h}_{\text{hf},i}$ are the local dipole and induced hyperfine fields on the nitrogen ion produced by the U ion located at the i position in the crystal lattice.

As described in the previous section, the main contribution to the induced magnetic field on the nitrogen nucleus in the paramagnetic phase is caused by the hyperfine field which is connected with the magnetism of the uranium 5f electrons via the H_f constant. At $T \gg T_N$ in the absence of correlation between the uranium magnetic moments the resulting local field on the nitrogen nuclei is directed along the external magnetic field. The dipole field $\mathbf{H}_{\text{dip}}$ with ten coordination spheres was calculated using a common expression [25,26,36,37]. According to these calculations, the dipole fields induced on a nitrogen nucleus by uranium ions equal zero in the paramagnetic phase at any magnetic field orientation with respect to the crystallographic axis of the UN single crystal. Consequently, the local field at the nitrogen nucleus is equal in magnitude to the algebraic sum of the hyperfine fields induced by the nearest uranium ions:

$$\mathbf{H}_{\text{loc}} = \mathbf{H}_{\text{hf}} = \sum_i \text{h}_{\text{hf},i} = \sum_i \mathbf{H}_{f,i}\boldsymbol{\mu}_{\mathbf{i}} = \mathbf{H}_f\boldsymbol{\mu}, \qquad (3)$$

where $\boldsymbol{\mu} = \boldsymbol{\mu}_i$ is the magnetic moment of the uranium ion in the Bohr magneton μ_B on the i position of the U ion and H_f is determined for the paramagnetic phase.

The uranium $5f$ electrons from the two first coordination spheres around the nitrogen nucleus contribute mainly to hyperfine field $\mathbf{H}_{\text{hf}}$. The first coordination sphere consists of six nearest uranium ions ($z_1 = 6$), the second one consists of eight ions ($z_2 = 8$). Expression (3) can be written as a sum:

$$\mathbf{H}_{\text{hf}} = (z_1 H_{f,1} + z_2 H_{f,2})\boldsymbol{\mu} = H_f\boldsymbol{\mu}, \qquad (4)$$

where $H_{f,1}$ and $H_{f,2}$ are the hyperfine fields produced at the location of nuclear probe ^{14}N by the uranium ions from the first and second coordination spheres, respectively. The values $H_{f,1}$ and $H_{f,2}$ can be estimated.

Generally speaking, there are three types of magnetic domains in the AF state UN [6,14]. Type *I* antiferromagnetic order with $1k$ structure is realized in each domain. In the UN cubic crystal lattice, the $1k$ structure implies ferromagnetic order of the magnetic moments in each plane, for example, (001), with the uranium magnetic moments being perpendicular to the planes. In turn, the planes alternate in such an order that magnetic moments in the adjacent planes are antiparallel $(\cdots\downarrow\uparrow\downarrow\uparrow\cdots)$. When an external magnetic field is applied, the magnetic equivalence of the nitrogen ions becomes broken inside each of the ordered AF domains [Figs. 4(c) and 5(c)]. Therefore, each domain deserves separate consideration.

Let us consider the case when a magnetic field is applied along the [111] direction [Fig. 5(c)]. In this case the U magnetic moments form an angle of 54.7 ° with the magnetic field in all domains and the domain structure remains invisible. Further, four out of six uranium ions from the first coordination sphere compensate their induced hyperfine fields $\mathbf{H}_{\text{hf}}$ [relation (3)] on the nitrogen ion while the other two do not. In the second coordination sphere, there is no compensation but the induced fields are against the field produced by the first coordination sphere. The dipole fields $\mathbf{H}_{\text{dip}}$ were calculated using the same calculation scheme as for the paramagnetic phase [25,26,36,37]. According to these calculations, dipole fields $\mathbf{H}_{\text{dip}} = 4.90\,\text{kOe}/\mu_\text{B}$ induced on the nitrogen ion lie along the direction of the ordered uranium magnetic moments and against the induced field $\mathbf{H}_{\text{hf}}$. Moreover, for the nitrogen ions the total fields $\mathbf{H}_{\text{loc}}$ [relation (2)] at positions N$_4$ and N$_5$ are equal in magnitude but opposite in direction; i.e., these positions become nonequivalent. It results to two lines, 4 and 5, in the ^{14}N NMR spectrum as observed in the experiment. Thus, for this case **B** ∥ [111], the following relation can be written as

$$\begin{aligned}(\nu_5 - \nu_4)/\gamma_n &= 2H_{\text{hf}} \\ &= 2|-2H_{f,1} + 8H_{f,2} + H_{\text{dip}}|\mu\cos(54.7^\circ). \end{aligned}\qquad (5)$$

Figure 5(b) shows that below 20 K the line splitting reaches a plateau $(\nu_5\text{–}\nu_4)_{\max} = 674\,\text{kHz}$, that corresponds to a maximum value of magnetic moment in the ordered state $\mu = \mu_{\text{ord}} = 0.75\,\mu_\text{B}$ [15].

From relation (5) we get the equation for hyperfine fields $H_{f,1}$ and $H_{f,2}$:

$$|-2H_{f,1} + 8H_{f,2} + 4.90| = 2.53\,\text{kOe}/\mu_\text{B}. \qquad (6)$$

By adding relation (4) to Eq. (6), we obtain as follows:

$$6H_{f,1} + 8H_{f,2} = 18.1\,\text{kOe}/\mu_\text{B}. \qquad (7)$$

Equations (6) and (7) give two solutions, namely, $^1H_{f,1}(\mathbf{B}\parallel[111])$=2.56 kOe/$\mu_\text{B}$, $^1H_{f,2}(\mathbf{B}\parallel[111])$=0.34 kOe/$\mu_\text{B}$ and $H_{f,1}(\mathbf{B}\parallel[111]) = 3.19\,\text{kOe}/\mu_\text{B}$, $H_{f,2}(\mathbf{B}\parallel[111]) =$ –0.13 kOe/μ_B. To determine which solution is correct, it is necessary to measure the ^{14}N NMR spectrum in the AF phase for different mutual orientations of the external magnetic field and the single crystal.

In the second case, with the magnetic field direction along the [001] (Fig. 4), the local field is also determined by the sum of hyperfine $\mathbf{H}_{\text{hf}}$ and dipole $\mathbf{H}_{\text{dip}}$ fields (relation 2). These fields on the nitrogen ion manifest themselves in the same way as in the case of **B** ∥ [111]. However, at **B** ∥ [001] not only the equivalence of nitrogen positions, but also of the magnetic domains is broken [Fig. 4(c)]. For domains in which the ordered uranium magnetic moments lie along the direction of magnetic field, projection of the total induced field $\mathbf{H}_{\text{hf}} + \mathbf{H}_{\text{dip}}$ on the external field direction at the N$_1$ and N$_3$ sites is of the same magnitude but of different sign. This results to two lines, 1 and 3, in the spectrum [Fig. 4(a)]. In the families of domains in which the magnetic moments of uranium are perpendicular to magnetic field, the projection of the $\mathbf{H}_{\text{hf}} + \mathbf{H}_{\text{dip}}$ field on the magnetic field direction is zero, so the line shift does not occur. This results in the appearance of the additional line 2 in the spectrum [Fig. 4(a)]. Therefore, at **B** ∥ [001] three lines are observed in the ^{14}N NMR UN spectrum.

To calculate the values of $H_{f,1}$ and $H_{f,2}$ for the **B** ∥ [001], the external field orientation, the following relation can be written:

$$\begin{aligned}(\nu_3 - \nu_1)/\gamma_n &= 2(H_{\text{hf}} + H_{\text{dip}}) \\ &= 2|-2H_{f,1} + 8H_{f,2} + H_{\text{dip}}|\mu. \end{aligned}\qquad (8)$$

By adding relation (4) to relation (8), we obtain as follows:

$$6H_{f,1} + 8H_{f,2} = 16.2\,\text{kOe}/\mu_\text{B}. \qquad (9)$$

Figure 4(b) shows that at **B** ∥ [001] the maximum splitting of lines 1 and 3 is $(\nu_3 - \nu_1)_{\max} = 200\,\text{kHz}$. Then Eqs. (8) and (9) give two estimates, namely, $^1H_{f,1}$ $(\mathbf{B}\parallel[001]) = 2.58\,\text{kOe}/\mu_\text{B}$, $^1H_{f,2}$ $(\mathbf{B}\parallel[001]) = 0.10\,\text{kOe}/\mu_\text{B}$ and $^2H_{f,1}$ $(\mathbf{B}\parallel[001]) = 2.69\,\text{kOe}/\mu_\text{B}$, $^2H_{f,2}$ $(\mathbf{B}\parallel[001]) = 0.01\,\text{kOe}/\mu_\text{B}$. Comparison of the estimates obtained for the orientations of external field **B** ∥ [111] and **B** ∥ [001] shows that the values of $^1H_{f,1}$ and $^1H_{f,2}$ are closer in both cases than the values of $^2H_{f,1}$ and $^2H_{f,2}$. Though the origin of hyperfine fields $H_{f,1}$ and $H_{f,2}$ is not well studied on the microscopic scale, their estimates reveal the following important circumstances. First, there exists the relation $|H_{f,1}| \gg |H_{f,2}|$. Second, the ^{14}N NMR spectrum in the AF phase is well explained within the framework of the AF ordering model of type *I*, which corresponds to the $1k$ structure in the presence of magnetic domains.

Recently, the issue of magnetic domain structure was raised in Ref. [6]. It is suggested that at the critical magnetic field $B_{C1} \approx 100\,\text{kOe}$ the magnetic domains rearrange and align along the magnetic field direction. This effect can cause magnetostriction and change of the electrical resistivity, as well as hysteresis between up- and down-field sweep. In our NMR experiment the sample was cooled down in the constant magnetic field of 92.8 kOe, which is slightly less than the critical field $B_{C1} \approx 100\,\text{kOe}$. Let us consider our result obtained with the field applied along the [001] direction and compare the sum of the integral intensities of lines 1 and 3 (both correspond to the left domain scheme in Fig. 4) with the integral intensity of line 2 (right domain scheme in Fig. 4). The obtained intensity ratio is about 1.6. This means that the number of domains with magnetic moments directed along the magnetic field is about 1.6 times higher than the number of domains with magnetic moments directed perpendicular to the field. As soon as the field in our experiment is less than B_{C1}, the domain rearrangement is not complete. Similar effects of the coexistence of several magnetic structures in the transition temperature range are well known (see, e.g., [36,38]. Thus our results do not contradict the results of [6]. On the contrary, they seem to be complementary to those of Ref. [6]. In the case of a magnetic field along the [111] direction, magnetic domains are not distinguishable, so that it is not possible to follow the domain rearrangement process.

C. Spin-lattice relaxation rate of T_1^{-1} of ^{14}N nuclei and f electron spin dynamics

In this section the measurement results of the ^{14}N nuclei spin-lattice relaxation rate T_1^{-1} are considered to probe the low-frequency dynamics of the f electrons in both paramagnetic and AF phases of UN.

Figure 6(a) shows the spin-lattice relaxation rate for the UN single crystal measured within the temperature range $T_N < T \leqslant 380\,\text{K}$ in magnetic field $\mathbf{B} \parallel [001]$ and for polycrystalline UN within a wider temperature interval up to 760 K. Note that the T_1^{-1} values are very close for both samples at temperatures between T_N and 380 K. This can be an evidence for the T_1^{-1} isotropy along all the crystallographic directions. Two features of the T_1^{-1} vs T curves should be mentioned. First, the temperature dependences of T_1^{-1} look rather unusual, since T_1^{-1} does not practically change above T_N. T-independent behavior of T_1^{-1} in UN [see also Fig. 6(b)] differs remarkably from that observed for the isostructural compounds UP ($T_N = 122\,\text{K}$) [39] and UAs ($T_N = 126\,\text{K}$) [40]. In these materials evident growth of T_1^{-1} is found for the ^{31}P and ^{75}As nuclei, respectively, when the temperature decreases and approaches T_N. Second, as mentioned in Ref. [20], the product $(^{14}T_1\,T)^{-1}$ in UN is more than an order of magnitude larger than $(^{14}\gamma\,/\,^{15}\gamma)^2(^{15}T_1\,T)^{-1} \approx 6 \times 10^{-4}(\text{s K})^{-1}$ in Th ^{15}N [29]. In Th ^{15}N the spin-lattice relaxation rate of the ^{15}N nuclei is governed by the Korringa mechanism, i.e., the Fermi contact interaction with conduction electrons [41]. Comparison of UN with ThN points out that the spin-lattice relaxation rate in the paramagnetic UN phase is determined by the $T_{1,f}^{-1}$ contribution caused by the time-dependent isotropic part of induced hyperfine interaction $\gamma_n \hbar \mathbf{I} H_f \Sigma_j \mathbf{S}_j^f(t)$ between the nitrogen nuclear momentum $\gamma_n \hbar \mathbf{I}$ and spin $\mathbf{S}_j^f(t)$ of the uranium 5f electrons [42]. Following [43] and summing up the contributions from the nearest uranium ions alone, we obtain as follows:

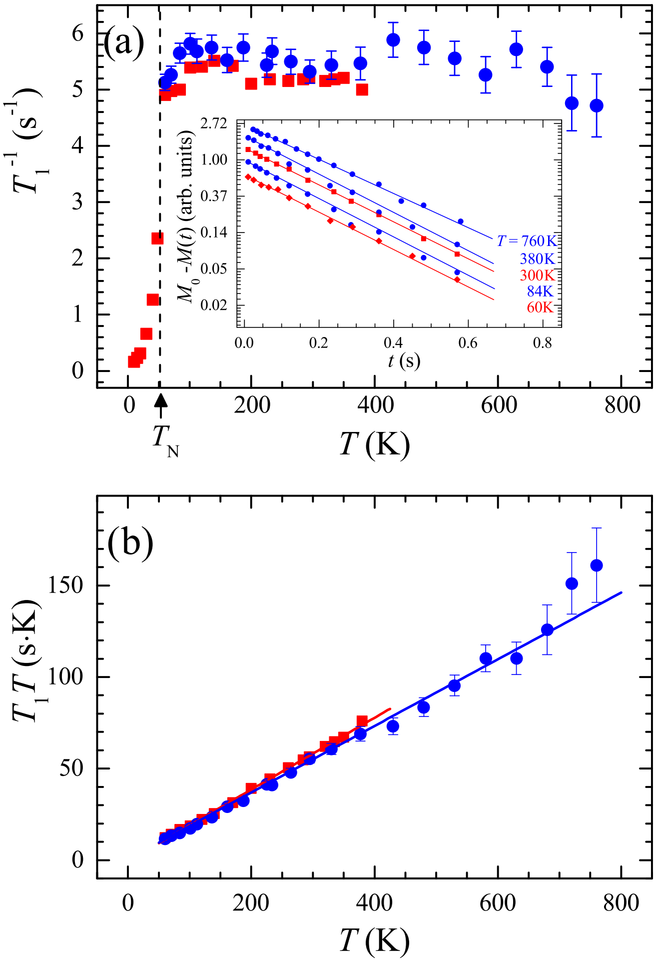

FIG. 6. (a) Spin-lattice relaxation rate T_1^{-1} of the ^{14}N nuclei as a function of temperature in the paramagnetic phase of UN for polycrystalline sample (circles) and single crystal at $\mathbf{B} \parallel [001]$ (squares). The inset shows the intensity of spin-echo signal $M(t)$ vs time t at different temperatures. Note logarithmic scale of the $M(t)$ axis. Solid lines represent fitting to the data by the $[M_0 - M(t)] \propto \exp(-tT_1^{-1})$ dependence. (b) The same T_1^{-1} data plotted as T_1T vs T for (squares) single and (circles) polycrystalline samples. Solid lines represent linear fit of the experimental points to emphasize almost stable T_1 values within wide temperature intervals. Large point scattering at $T = 720\,\text{K}$ and 760 K for polycrystalline sample is due to weak echo signals.

$$T_{1,f}^{-1} = \frac{2\gamma_n^2 k_B T}{\mu_B^2} H_f^2 \sum_q [\cos(q_x a) + \cos(q_y a) + \cos(q_z a)]^2 \times \frac{\chi''{}_f(q, \omega_n)}{\omega_0}, \tag{10}$$

where k_B and $\hbar$ are Boltzmann and Planck constants, respectively; $\chi''(q, \omega_n)$ is the imaginary part of the 5f-electron spin susceptibility at NMR frequency ω_0; and the hyperfine field H_f does not depend on the wave vector $\mathbf{q}$ of magnetic excitations. The magnitude and temperature dependence of $T_{1,f}^{-1}$

are determined mainly by the localization degree of the $5f$ electrons.

If one assumes the delocalized nature of the $5f$ electrons which form weak antiferromagnetic metal [44], strong temperature dependence of magnetic susceptibility in UN could be connected with formation of a narrow $\sim k_B\theta$ peak of the $5f$ density of state near the Fermi energy. In this case partial hybridization of the itinerant $5f$-$6d$ states affects only the Korringa contribution to the ^{14}U nuclei spin-lattice relaxation rate $(T_1^{-1})_K \propto T$. In the case of an itinerant magnet with "nearly localized" $5f$ electrons the product $(T_1T)^{-1}$ should be proportional to $1/(T{-}T_N)^{0.5}$ (see, e.g., [45] and references therein). Namely, such a behavior is observed in UP [39] and UAs [40]. However, our spin-relaxation data show that in UN T_1T is proportional to T [Fig. 6(b)]; i.e., $(T_1T)^{-1} \sim 1/T$, not to $1/(T{-}T_N)^{0.5}$ (see also Fig. 5(b) in Ref. [20]).

Since the behavior of the spin-lattice relaxation time in UN differs from that expected in itinerant magnetic systems, it is useful to consider the case of localized $5f$ states. For the completely localized U $5f$ electrons at $T \gg T_N$ the exchange-coupled magnetic moments of neighbor $U^{3+}(5f^3)$ ions fluctuate independently of each other. In this case, the maximum value of rate $(T_1^{-1})_{f,T\to\infty}$ is determined by the exchange interaction energy $\hbar\omega_{ex}$:

$$\left(T_{1,f}^{-1}\right)_{T\to\infty} = (2\pi\gamma_n g J\mu_B H_{f,1})^2 zJ(J+1)/3\omega_{ex}, \qquad (11)$$

where J is the full angular momentum of the U ion, and g_J is the Landé factor.

Approximating experimental magnetic susceptibility $\chi(T)$ by the Curie-Weiss dependence and using the molecular field expression for ω_{ex} [46], we obtain as follows:

$$(\hbar\omega_{ex})^2 = (k_B\theta)^2 3g_J[z|g_J-1|^3 J(J+1)]^{-1}, \qquad (12)$$

where $z = z_1$ is the number of the nearest neighbors. Equation (11) gives the estimates $\omega_{ex}(U^{3+}; 5f^3) = 2.2 \times 10^{13}\ s^{-1}$ and $\omega_{ex}(U^{4+}; 5f^2) = 4.1 \times 10^{13}\ s^{-1}$ corresponding to the values of $(T_1^{-1})_{f,T\to\infty} = 70\ s^{-1}$ and $37\ s^{-1}$.

These values exceed significantly the experimentally measured rates $T_1^{-1} \approx 5\ s^{-1}$ at 380 K for the single and at 760 K for the polycrystalline UN samples (Fig. 6) [47]. Since these estimations indicate a downward trend of $(T_1^{-1})_{f,T\to\infty}$ with a decrease of the U $5f$ shell population, to understand the mechanism responsible for unusually low spin-lattice relaxation rate T_1^{-1} in UN, let us focus on the compounds with fluctuating valence (and, accordingly, magnetic moments) states of an actinide ion [10,48]. In these materials the characteristic spin fluctuation energy $\Gamma(q)$ corresponds to the half width at half maximum of Lorentzian $\chi''(q,\omega) = \chi(q)\omega\Gamma(q)/[\omega^2 + \Gamma(q)^2]$, which describes the low-frequency part of the magnetic spectrum measured by inelastic neutron scattering experiments [17]. Neglecting the correlation effects between the $5f$ electrons of the neighboring U ions, the expression for $\chi''(q,\omega)$ at the NMR frequencies $\omega_0 \ll \omega_{ex}$ is reduced to $\chi''(q,\omega_0) \approx \chi_f\omega_0/\Gamma_{nmr}$, where χ_f is the static magnetic susceptibility of the $5f$ electrons. Correspondingly, the general relation (10) for $T_{1,f}^{-1}$ is reduced to

$$T_{1,f}^{-1} = \gamma_n^2 k_B T z H_{f,1}^2 \chi_f / 2\mu_B^2 \Gamma_{nmr}. \qquad (13)$$

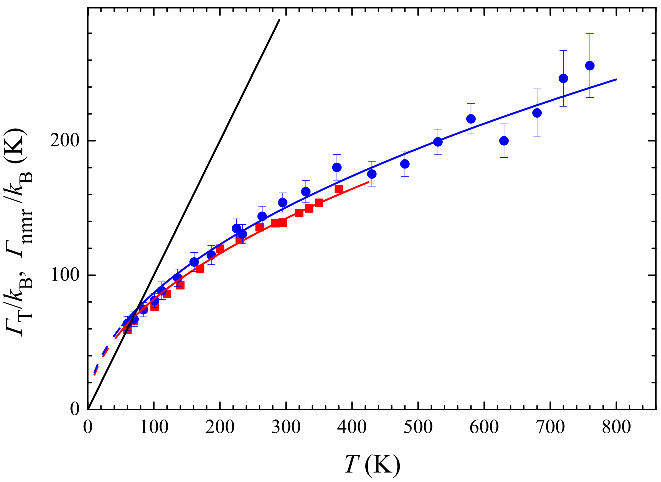

FIG. 7. Temperature dependence of the characteristic spin fluctuation energy $\Gamma_{nmr}/k_B \propto K_f T_{1,f} T$ (in temperature units) of the U $5f$ electrons for the UN single crystal (**B** ∥ [001], squares) and polycrystalline UN sample (circles). Solid lines represent the dependence $\Gamma_{nmr}(T) = \Gamma(0) + c\sqrt{T}$ with $\Gamma(0) = 0.5$ K for both curves and $c = 8.2$ and 8.7 for single and polycrystalline samples, respectively. Lines are extrapolated to zero temperature. Relation $\Gamma_{nmr}(T)/k_B = T$ is shown by a straight line.

Taking into account the NMR line shift $K_f = zH_f\chi_f/\mu_B$, the relation for $\Gamma_{nmr}(T)$ is as follows:

$$\Gamma_{nmr}(T) = \left(\gamma_n^2 k_B H_f / 2\mu_B\right) K_f T_{1,f} T. \qquad (14)$$

Relation (14) allows an estimation of the characteristic spin fluctuation energy of the $5f$ electrons using the NMR data. Figure 7 demonstrates that in the UN single crystal Γ_{nmr} increases monotonically with temperature and follows a power law which is rather close to the $\Gamma_{nmr}(T) \propto T^{0.5}$ dependence observed in the concentrated Kondo systems above the coherent state formation temperature [12,21]:

$$\Gamma_{nmr}(T) = \Gamma_{nmr}(0) + c\sqrt{T}, \qquad (15)$$

where $\Gamma_{nmr}(0)$ and c are constants. Similar power behavior of $\Gamma_{nmr}(T) \sim T^{0.5}$ is also observed up to $14T_N$ for the polycrystalline UN samples (Fig. 7).

Using relation (14), we obtain the estimation of spin fluctuation energy $\Gamma_{nmr}(300\ K) \approx 140$ K at room temperature, being of the same order of magnitude as the half width of the quasielastic line $\Gamma_{qe} \sim 2$–3 THz (or 100 – 140 K) of the neutron scattering spectrum in UN at 300 K [17]. The NMR experiments show that within the wide temperature range $1.5T_N < T < 14T_N$, Γ_{nmr} is less than $\Gamma_T = k_BT$ (Fig. 7). In other words, the characteristic time of thermal fluctuations $\tau_T = \hbar/k_BT$ is less than that of the magnetic fluctuations $\tau_{sf} = \hbar/2\Gamma_{nmr}$ in the paramagnetic phase of UN. In terms of the local moment regime of the $5f$ states, this behavior implies that fast thermal fluctuations dominate at $1.5T_N < T < 14T_N$ leading to the Curie-Weiss behavior of the Knight shift and magnetic susceptibility, while the spin-lattice relaxation is governed by magnetic fluctuations [12,21]. According to [21], the $T^{0.5}$ law is valid in the valence-fluctuation compounds for $6 < T/T_0 < 100$, while $\Gamma(T)$ becomes nearly temperature independent below T_0. Namely, such a behavior is found for an archetype heavy fermion system $CeAl_2$, the quasielastic linewidth vs T curve of which resembles the $\Gamma_{\mathrm{nmr}}(T)$ vs T curve in Fig. 7 [49]. The Néel temperature of $CeAl_2$ is 3.8 K and $\Gamma(0)$ is approximately 0.5 meV [50]. In UN the AF transition occurs at $T_{\mathrm{N}} = 51$ K, making it impossible to determine the low-temperature limit of the $T^{0.5}$ law validity and $\Gamma(0)$. Since the lowest temperature of the T_1 measurements in the paramagnetic regime is 60 K in our experiments, the T_0 value must be at least below $\sim$60/6, i.e., below 10 K.

As known [12], the ground state of valence-fluctuating f-electron systems is determined by the interplay between the two competing processes, the indirect exchange interaction of f-shell ions via the Ruderman–Kittel–Kasuya–Yosida (RKKY) oscillations, and the effective suppression of magnetic moments due to the Kondo spin fluctuations. If the Kondo temperature T_{K} is much higher than the RKKY temperature T_{RKKY}, under decreasing temperature a crossover should occur to the $\tau_{\mathrm{sf}} < \tau_{\mathrm{T}}$ regime and, in the limit $T \to 0$, the local magnetic moment of the f shell should be effectively suppressed by Kondo fluctuations and the system becomes a Fermi liquid (FL) with a large effective mass. The situation with $T_{\mathrm{K}} \geqslant T_{\mathrm{RKKY}}$ and nonzero temperature of magnetic order corresponds to the magnetic ground state, essentially modified because of the Kondo compensation of the localized magnetic moment of the f-shell ions. In this case decreasing temperature leads to the Kondo effect, but transition to a magnetically ordered state precedes formation of a nonmagnetic singlet ground state. The above-mentioned $CeAl_2$ is a typical example of such magnetic concentrated Kondo systems (CKS). In UN the crossover $\Gamma_{\mathrm{nmr}}/k_{\mathrm{B}} > T$ occurs near T_{N} (Fig. 7), and the dominance of Kondo fluctuations $\tau_{\mathrm{sf}} = \hbar/2\Gamma_{\mathrm{nmr}} < \tau_{\mathrm{T}} = \hbar/k_{\mathrm{B}}T$ is expected at lower temperatures, in the absence of the AF transition. Thus, according to our NMR and magnetic susceptibility measurements, UN can be classified as a magnetic CKS, with an anomalously small sublattice magnetic moment $\mu_{\mathrm{ord}} = 0.75\,\mu_{\mathrm{B}}$ in the AF state [15] which can be associated with the screening effect due to anomalous spin fluctuations.

Investigation of the ^{14}N nuclei spin-lattice relaxation rate nearby and below the Neél temperature is of special interest. Measurements of the ^{14}N nuclei spin-lattice relaxation rate T_1^{-1} for the UN single crystal in magnetic field $\mathbf{B} \parallel [001]$ show that T_1^{-1} is proportional to temperature below $T_{\mathrm{N}}/2$ (Fig. 8); that is, Korringa's law $T_1^{-1}(T) \propto TN^2(E_{\mathrm{F}})$ is valid [50]. This is the evidence of formation of the FL state with band width $W \gg k_{\mathrm{B}}T$ [35,41].

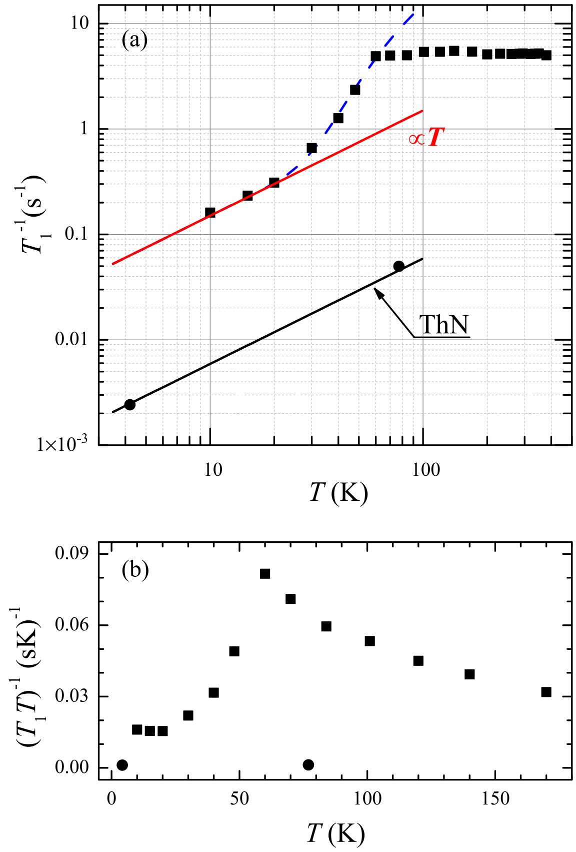

FIG. 8. (a) The T_1^{-1} vs T dependence for the UN single crystal below T_{N} at $\mathbf{B} \parallel [001]$ (squares) and for ThN (circles) [29]. Note logarithmic scale of both axes. Solid lines are the linear fit of the T_1^{-1} data (a guide for the eye). The dashed line is the fitting to the data by expression (15). (b) The same data plotted as $(T_1T)^{-1}$ vs T.

Figures 8(a) and 8(b) show also the spin-lattice relaxation rate vs temperature data for the ^{14}N nuclei in ThN at low temperatures [29]. There are no f electrons in ThN, and T_1^{-1} is 25 times lower than in UN. This is evidence of the $5f$ uranium electrons' responsibility for the relaxation of nitrogen nuclear moments in UN down to the lowest temperatures. The gap character of the T_1^{-1} temperature dependence within the temperature interval $T_{\mathrm{N}}/2 < T < T_{\mathrm{N}}$ is to be noted. Such a gaplike behavior of the UN electrical resistivity is observed in [5], the value of the magnon energy gap being $\Delta = 165$ K. To estimate the gap value our T_1^{-1} vs T data are approximated as follows:

$$T_1^{-1} = C \times \exp(-\Delta/T) + D \times T, \qquad (16)$$

where C and D are constants. Our data can be well approximated with the value of $\Delta = 180$ K close to $\Delta = 165$ K from Ref. [5], as well as to the value of the anisotropy gap $\sim$16 meV$\sim$185 K [17]. Although measurements of the spin-lattice relaxation rate are absent between $T = 60$ K and T_{N}, we believe that a sudden change in T_1^{-1} within this temperature interval results from the gap opening in the magnetic excitation spectrum, while the $5f$ electrons still dominate the spin dynamics of UN.

Thus the results of our NMR and magnetic susceptibility experiments are compatible with the description of UN in terms of localized magnetic moment behavior at T above T_{N}. However, this conclusion contradicts numerous experimental and calculation results that emphasize the itinerant nature of the f electrons in UN [1–6]. Particularly, Fujimori *et al.* on the basis of ARPES data and band-structure calculations conclude that an itinerant description of the U $5f$ states is appropriate for UN, while the dual nature of U $5f$ electrons is not observed in their experiment [8]. On the other hand, according to the LDA+DMFT calculation by Yin *et al.* [10], the actinides ions in most of the metallic crystals are found to be in a mixed valence state, where they fluctuate between different valences. It can be described by an effective f-electron valence n_f ($n_f = 2.4$ in the case of UN). A characteristic energy scale of the order of 1700 K (the authors call it the Kondo temperature) is required to describe UN electrical resistivity. According to [10], UN is a non-FL in the temperature range 55–1000 K, and shows a strongly correlated heavy fermion character with a coherence temperature below its Neél temperature. In the absence of magnetic order, UN would be a Fermi liquid at very low temperature with large mass enhancement [10]. Our results demonstrate that the FL state is formed in the AF state of UN. Although Yin *et al.* [10] do not discuss the magnetic properties of UN, the characteristic energy scale ~1700 K may, in principle, explain the absence of measurable crystal field excitations and partial μ_{eff} compensation above T_N. It is not obvious whether the behavior of the spin-lattice relaxation rate in UN observed in our experiments can also be explained in terms of the same approach. Therefore, an appropriate theoretical framework for UN description, including its magnetic properties, is still not known. The problem of dual localized-itinerant behavior of the $5f$ electrons in UN remains an open question [5]. Besides, it is worth noting that the multiconfigurational nature of the $5f$ orbitals is not a rarity in U- and Pu-based intermetallics [51]. Hence, we cannot exclude that the ground state of UN is a quantum superposition of more than two $5f$ electronic configurations of the U ions and fluctuations between these configurations are responsible for the contradictory properties of UN [20]. Obviously, this issue requires additional study.

IV. CONCLUSIONS

The ^{14}N NMR technique is employed to study spin susceptibility and low-frequency dynamics of the uranium $5f$ electrons in paramagnetic and magnetically ordered phases for the UN single crystal ($T_N = 51 \pm 1$ K) and polycrystalline UN sample ($T_N = 53 \pm 1$ K). In the paramagnetic region the ^{14}N NMR line shift $K(T)$, as well as the full magnetic susceptibility $\chi(T)$, follow the Curie-Weiss law up to 760 K. It is shown that the main contribution to both $K(T)$ and $\chi(T)$ in the paramagnetic UN phase is connected with the $5f$-electron local moment magnetism of six uranium ions nearest to nitrogen. Almost constant spin-lattice relaxation time T_1 is observed within the temperature range from 760 to 60 K. The characteristic spin fluctuation energy Γ_{nmr} of $5f$ electrons increases monotonically with increasing temperature according to the power law, which almost exactly coincides with the dependence $\Gamma(T) \propto T^{0.5}$, observed in the concentrated Kondo systems above the coherent state formation temperature. According to our estimations, in the paramagnetic phase the energy of anomalous spin fluctuations Γ_{nmr} is less than $k_B T$, but, as the measurements on the UN single crystal show, Γ_{nmr}/k_B becomes equal to T near the transition to the antiferromagnetic state. Therefore, below the Neél temperature the dominance of magnetic fluctuations $\tau_{\text{sf}} = \hbar/2\Gamma_{\text{nmr}} < t_T = \hbar/k_B T$ is expected, if the AF transition does not occur. Besides, we find that Korringa's law $T_1^{-1}(T) \propto T$ is valid below $T \approx T_N/2$ by measuring the spin-lattice relaxation rate of the ^{14}N nuclei in the UN single crystal in magnetic field $\mathbf{B} \parallel [001]$. This is unambiguous evidence of formation of the Fermi liquid state in UN at low temperatures. The nature of this Fermi liquid state requires further study. Finally, we conclude that above T_N, UN clearly displays the features of a magnetic concentrated Kondo system. This conclusion contradicts the pure itinerant description of the U $5f$ states in UN and can be considered as an argument in favor of the multiconfigurational nature of the $5f$ orbitals in this compound.

A few lines are observed in the ^{14}N NMR spectrum in the AF phase. The positions and number of spectral lines depend on sample orientation with respect to the external magnetic field. The presence of several lines in the ^{14}N NMR spectrum indicates the existence of antiferromagnetic domains in the UN single crystal. The argument in favor of this statement is that application of an external magnetic field along different crystallographic directions leads to different shapes of the NMR spectra due to nonequivalence of orientation of the ordered U magnetic moments relative to the external field. Therefore, the peculiarities of the NMR spectra in the AF phase of UN can be explained in terms of the antiferromagnetic order of type *I* corresponding to the $1k$ structure in the presence of magnetic domains.

ACKNOWLEDGMENTS

The work was supported by the Russian Science Foundation (Project No. 18-72-10022). A.V.A. thanks the Czech Science Foundation (Project No. 19-00925S) and MGML [52] within the Program of Czech Research Infrastructures (Project No. LM2018096) for support in preparation of the single crystal for measurements. The work of Y.V.P. on the calculation of the spin fluctuation energy was carried out within the state assignment of Ministry of Science and Higher Education of the Russian Federation (theme "Function" No. AAAA-A19-119012990095-0).

---

[1] R. Troć, in *Pnictides and Chalcogenides III (Actinide Monopnictides)*, edited by H. P. J. Wijn, Landolt-Börnstein, New Series, Group III Vol. 27 (Springer, Berlin, 2006).

[2] A. Solontsov and V. P. Silin, Uranium nitride—a spin polarized weak itinerant electron antiferromagnet with strongly correlated electrons, Phys. Lett. A **334**, 453 (2005).

[3] K. G. Gurtovoi and R. Z. Levitin, Magnetism of actinides and their compounds, Sov. Phys. -Usp. **30**, 827 (1987).

[4] P. R. Norton, R. L. Tapping, D. K. Creber, and W. J. L. Buyers, Nature of the $5f$ electrons in uranium nitride: A photoelectron spectroscopic study of UN, U, UO$_2$, ThN, and Th, Phys. Rev. B **21**, 2572 (1980).

[5] M. Samsel-Czekala, E. Talik, P. de V. Du Plessis, R. Troc, H. Misiorek, and C. Sulkowski, Electronic structure and magnetic and transport properties of single-crystalline UN, Phys. Rev. B **76**, 144426 (2007).

[6] K. Shrestha, D. Antonio, M. Jaime, N. Harrison, D. S. Mast, D. Safarik, T. Durakiewicz, J.-C. Griveau, and K. Gofryk, Tricritical point from high-field magnetoelastic and metamagnetic effects in UN, Sci. Rep. **7**, 6642 (2017).

[7] H. H. Hill, Plutonium 1970 and other actinides,nuclear metallurgy, in *Proceedings of the 4th International Conference*, edited by W. N. Miner (American Institute of Mining, Metallurgical, and Petroleum Engineers, New York, 1970), Vol. 17, p. 2.

[8] S.-i. Fujimori, T. Ohkochi, T. Okane, Y. Saitoh, A. Fujimori, H. Yamagami, Y. Haga, E. Yamamoto, and Y. Onuki, Itinerant nature of U $5f$ states in uranium mononitride revealed by angle-resolved photoelectron spectroscopy, Phys. Rev. B **86**, 235108 (2012).

[9] J. M. Fournier, J. Beille, A. Boeuf, C. Vettier, and A. Wedgwood, Magnetic structure of UN under pressure, Physica B+C (Amsterdam) **102**, 282 (1980).

[10] Q. Yin, A. Kutepov, K. Haule, G. Kotliar, S. Y. Savrasov, and W. E. Pickett, Electronic correlation and transport properties of nuclear fuel materials, Phys. Rev. B **84**, 195111 (2011).

[11] A. V. Lukoyanov and V. I. Anisimov, Electronic structure of nitrides PuN and UN, J. Exp. Theor. Phys. **123**, 864 (2016).

[12] N. B. Brandt and V. V. Moshchalkov, Concentrated Kondo systems, Adv. Phys. **33**, 373 (2006).

[13] R. Troć, Magnetic susceptibility of the uranium nitrides, J. Solid State Chem. **13**, 14 (1975).

[14] C. F. van Doorn and P. de V. du Plessis, Magnetic properties of single-crystal uranium mononitride, J. Low Temp. Phys. **28**, 391 (1977).

[15] N. A. Curry, An investigation of the magnetic structure of uranium nitride by neutron diffraction, Proc. Phys. Soc. **86**, 1193 (1965).

[16] J. Grunzweig-Genossar, M. Kuznietz, and F. Friedman, Magnetic properties of uranium compounds with elements of the V*A* and VI*A* groups. I. Compounds of U*X* type, Phys. Rev. **173**, 562 (1968).

[17] T. M. Holden, W. J. L. Buyers, E. C. Svensson, and G. H. Lander, Magnetic excitations in uranium nitride, Phys. Rev. B **30**, 114 (1984).

[18] M. Kuznietz, NMR of ^{14}N in the paramagnetic state of uranium mononitride, Phys. Rev. **180**, 476 (1969).

[19] M. Kuznietz and D. O. van Ostenburg, Nuclear magnetic resonance of ^{15}N in the paramagnetic state of enriched uranium mononitride (U ^{15}N), Phys. Rev. B **2**, 3453 (1970).

[20] V. V. Ogloblichev, A. M. Potapov, S. V. Verkhovskii, and A. V. Mirmelstein, ^{14}N Nuclear magnetic resonance and relaxation in the paramagnetic region of uranium mononitride, JETP Lett. **108**, 616 (2018).

[21] D. L. Cox, N. E. Bickers, and J. W. Wilkins, Dynamic magnetic susceptibilities of valence-fluctuation Ce compounds, J. Appl. Phys. **57**, 3166 (1985).

[22] D. I. Gorbunov, T. Nomura, A. A. Zvyagin, M. S. Henriques, A. V. Andreev, Y. Skourski, G. A. Zvyagina, R. Troc, S. Zherlitsyn, and J. Wosnitza, Magnetoelastic coupling across the field-induced transition of uranium mononitride, Phys. Rev. B **100**, 024417 (2019).

[23] R. Troc, M. Samsel-Czekała, A. Pikul, A. V. Andreev, D. I. Gorbunov, Y. Skourski, and J. Sznajd, Electronic structure of UN based on specific heat and field-induced transitions up to 65 T, Phys. Rev. B **94**, 224415 (2016).

[24] L. A. O'Dell, Direct detection of nitrogen-14 in solid-state NMR spectroscopy, Prog. Nucl. Magn. Reson. Spectrosc. **59**, 295 (2011).

[25] A. Abragam, *The Principles of Nuclear Magnetism* (Clarendon Press, Oxford, 1961).

[26] C. P. Slichter, *Principles of Magnetic Resonance* (Harper & Row, New York, 1963).

[27] Suppose that in a not ideal cubic crystal lattice the main axis of EFG eV_{zz} lies along the crystal direction [001] while the asymmetry parameter $\eta = (V_{yy}–V_{xx})/V_{zz}$ is very small. Then, in the case of $\mathbf{B} \parallel [111]$ the angle between the direction of B and the main axis of EFG, $\Theta = 54.7^\circ$, so that the quadrupole effects equal zero [25,26]. In the case of $\mathbf{B} \parallel [001]$, [010], and [100] angle $\Theta = 90^\circ$ or 180° and the quadrupole interaction is not zero leading to the ^{14}N NMR line broadening.

[28] M. Kuznietz, NMR properties of ^{14}N in ThN and of ^{31}P in ThP, J. Chem. Phys. **49**, 3731 (1968).

[29] J. L. Boutard, C. H. de Novion, and H. Alloul, ^{13}C and ^{15}N N.M.R. in thorium carbides and carbonitrides, J. Phys. (Paris) **41**, 845 (1980).

[30] J. Staun Olsen, L. Gerward, and U. Benedict, A new high-pressure phase of uranium nitride studied by x-ray diffraction and synchrotron radiation, J. Appl. Crystallogr. **18**, 37 (1985).

[31] C.-H. de Novion and P. Costa, Propriétés électroniques des carbonitrures d'uranium U(C1–xNx), J. Phys. (Paris) **33**, 257 (1972).

[32] R. H. Lemmer and J. E. Lowther, Magnetic properties of uranium monopnictides, J. Phys. C: Solid State Phys. **11**, 1145 (1978).

[33] H. Hasegawa and T. Moriya, Effect of spin fluctuation on itinerant electron antiferromagnet, J. Phys. Soc. Jpn. **36**, 1542 (1974).

[34] A. Freeman and R. Frankel, *Hyperfine Interactions* (Academic Press, New York, 1967).

[35] J. Winter, *Magnetic Resonance in Metals* (Oxford University Press, New York, 1971).

[36] V. V. Ogloblichev, A. F. Sadykov, Y. Furukawa, Q. P. Ding, A. G. Smolnikov, Y. V. Piskunov, K. N. Mikhalev, A. P. Gerashenko, A. Wu, S. N. Barilo, and S. V. Shiryaev, ^{63,65}Cu NMR study of the magnetically ordered state of the multiferroic CuFeO$_2$, J. Magn. Magn. Mater. **504**, 166668 (2020).

[37] V. V. Ogloblichev, A. G. Smolnikov, A. F. Sadykov, Y. V. Piskunov, A. P. Gerashenko, K. Kumagai, Y. Furukawa, A. Y. Yakubovsky, K. N. Mikhalev, S. N. Barilo, S. V. Shiryaev, and A. S. Belozerov, ^{17}O NMR study of the triangular lattice antiferromagnet CuCrO$_2$, J. Magn. Magn. Mater. **458**, 1 (2018).

[38] A. Yu. Germov, K. N. Mikhalev, S. V. Verkhovskii, Z. N. Volkova, A. P. Gerashchenko, A. V. Korolev, E. I. Konstantinova, I. A. Leonidov, and V. L. Kozhevnikov, Inhomogeneous magnetic state in the electron-doped Sr$_{0.98}$La$_{0.02}$MnO$_3$ manganite according to ^{55}Mn NMR data, JETP Lett. **102**, 727 (2015).

[39] S. Takagi, N. Niitsuma, T. Yoshida, and T. Kasuya,^{31}P nuclear magnetic relaxation studies of the dynamical magnetic behavior of UP, J. Phys. Soc. Jpn. **56**, 2287 (1987).

[40] H. Suzuki, S. Takagi, K. Mattenberger, and O. Vogt, Spin dynamics of UAs in the paramagnetic state as studied by ^{75}As NMR, Phys. B (Amsterdam, Neth.) **186–188**, 755 (1993).

[41] J. Korringa, Nuclear magnetic relaxation and resonance line shift in metals, Physica **16**, 601 (1950).

[42] A. Narath, in *Hyperfine Interactions*, edited by A. J. Freeman, and R. B. Frankel (Academic Press Inc., New York, 1967).

[43] T. Moriya, The effect of electron-electron interaction on the nuclear spin relaxation in metals, J. Phys. Soc. Jpn. **18**, 516 (1963).

[44] T. Moriya, *Spin Fluctuations in Itinerant Electron Magnetism* (Springer, Berlin, 1985).

[45] M. Corti, F. Carbone, M. Filibian, Th. Jarlborg, A. A. Nugroho, and P. Carretta, Spin dynamics in a weakly itinerant magnet from ^{29}Si NMR in MnSi, Phys. Rev. B **75**, 115111 (2007).

[46] T. Moriya, Nuclear magnetic relaxation in antiferromagnetics, Prog. Theor. Phys. **16**, 23 (1956).

[47] Note that in the case of U^{5+} ($5f^1$, $g_J = 0.86$, $J = 5/2$) configuration $\mu_{\text{eff}} = 2.5\,\mu_B$ is very close to $\mu_{\text{eff}} = 2.7\,\mu_B$ derived from the magnetic susceptibility measurements, but even in this case the estimate $1/T_1 \approx 15\,\text{s}^{-1}$ is still 3 times higher than the experimental value $1/T_1 \approx 5\,\text{s}^{-1}$. A similar $1/T_1$ estimate may be obtained also with the values of g and μ_{eff} obtained in Ref. [11].

[48] E. S. Clementyev and A. V. Mirmelstein, Kondo universality, energy scales, and intermediate valence in plutonium, J. Exp. Theor. Phys. **109**, 128 (2009).

[49] E. Holland-Moritz and G. H. Lander, Neutron inelastic scattering from actinides and anomalous lanthanides, in *Handbook on the Physics and Chemistry of Rare Earths*, edited by G. R. Choppin, K. A. Gschneidner, L. Eyring, and G. H. Lander (North-Holland, Amsterdam, 1994), Vol. 19, Chap. 130, p. 79.

[50] E. Holland-Moritz and G. H. Lander, Neutron inelastic scattering from actinides and anomalous lanthanides, in *Handbook on the Physics and Chemistry of Rare Earths*, edited by G. R. Choppin, K. A. Gschneidner, L. Eyring, and G. H. Lander, (North-Holland, Amsterdam, 1994), Vol. 19, Chap. 130, p. 78.

[51] C. H. Booth, Y. Jiang, D. L. Wang, J. N. Mitchell, P. H. Tobash, E. D. Bauer, M. A. Wall, P. G. Allen, D. Sokaras, D. Nordlund, T.-C. Weng, M. A. Torrez, and J. L. Sarrao, Multiconfigurational nature of $5f$ orbitals in uranium and plutonium intermetallics, Proc. Natl Acad. Sci. USA **109**, 10205 (2012).

[52] https://mgml.eu.